JACS
JOURNAL OF THE AMERICAN CHEMICAL SOCIETY

Article

pubs.acs.org/JACS

Enantio- and Regioselective Epoxidation of Olefinic Double Bonds in Quinolones, Pyridones, and Amides Catalyzed by a Ruthenium Porphyrin Catalyst with a Hydrogen Bonding Site

Philipp Fackler, Stefan M. Huber, and Thorsten Bach*

Lehrstuhl für Organische Chemie I and Catalysis Research Center (CRC), Technische Universität München, D-85747 Garching, Germany

Supporting Information

ABSTRACT: An array of differently substituted 3-alkenylquinolones was synthesized, and the enantio- and regioselectivity of their Ru-catalyzed epoxidation were studied. A precursor ruthenium(II) complex with a chiral tricyclic γ-lactam skeleton (octahydro-1*H*-4,7-methanoisoindol-1-one) was available by Sonogashira cross-coupling with a monobromo-substituted ruthenium(II) porphyrin. Enantioselective epoxidation reactions (60−83% yield, 85−98% *ee*) were achieved with this catalyst, and it was shown that the enantioselectivity depends critically on the presence of a two-point hydrogen bond interaction between the γ-lactam site of the catalyst and the δ-lactam (quinolone) site of the substrate. DFT calculations support the hypothesis that the reaction occurs via a hydrogen-bound transition state, in which the 3-alkenylquinolone adopts an s-*trans* conformation. The calculations further revealed that this transition state is preferred over a competing s-*cis* transition state because it exerts less strain in the rigid backbone and because the hydrogen bond interaction is more stable. The catalyst loading required for complete conversion was low (<0.2 mol %), and turnover numbers exceeding 4000 were recorded. It was shown that there is little, if any, inhibition of the catalytic process by other quinolones, which could potentially compete with the binding site. A mechanistic model for the catalytic reaction is presented. In accordance with this model 3-alkenylpyridones reacted with similar enantioselectivities as the respective quinolones. The epoxidation products were unstable, however, and the enantiomeric purity (77−87% *ee*) of the products could be established only after derivatization. Primary alkenoic acid amides also underwent the epoxidation but gave the respective products in lower enantioselectivities (70% and 45% *ee*), presumably because the enantioface differentiation is hampered by the increased flexibility of the substrates, which exhibit two or three rotatable single bonds between the binding site and the reactive olefinic double bond.

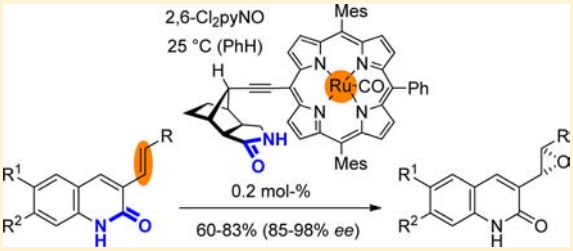

INTRODUCTION

Selectivity in transition-metal-catalyzed reactions is achieved by stabilization of a given transition state relative to other transition states, which lead to undesired reaction pathways. The complex nature of substrate and ligand coordination to a transition metal center[1] offers different approaches to selective transition metal catalysis. Among those approaches, the term supramolecular catalysis[2] describes the idea of using a supramolecular assembly[3] to influence or control the reactivity of one or more catalytically active centers. More specifically, supramolecular interactions in transition metal catalysis can be divided into ligand−ligand and ligand−substrate interactions.[4,5] Ligand−substrate interactions enable an indirect communication of the transition metal center with the substrate via the ligand. The ligand is crucial for selectivity because its supramolecular interaction with the substrate is responsible for the stabilization of a defined transition state. Since the ligand must bind to both the transition metal and the substrate it must be at least bifunctional.[6] Inspired by natural precedence,[7,8] hydrogen bonds are useful noncovalent interactions,[9] which enable supramolecular ligand−substrate binding and which have been successfully used to control the regioselectivity of a transition-metal-catalyzed reaction. Important examples of the use of bifunctional ligands in regioselective reactions[10] include the Ru-catalyzed hydration of alkynes,[11] the Mn-catalyzed C−H oxidation of ibuprofen and other carboxylic acids,[12] and the Rh-catalyzed hydroformylation of unsaturated carboxylic acids.[13] Enantioselectivity in supramolecular transition-metal-catalyzed reactions[14] has so far been mediated by hydrogen bonds only in larger entities, in which a *single* hydrogen bond is part of the ligand−substrate complex. An early example was presented by Gilbertson et al., who studied the Rh-catalyzed hydrogenation of certain olefins in the presence of peptides, which contained covalently bound phosphanes.[15] Reek et al. have shown the importance of hydrogen bonding in the enantioselective Rh-catalyzed hydrogenation with a leucine-derived phosphoramidite ligand (LEUPhos)[16] and with chiral amino acid derivatives as cofactors of achiral bisphosphane ligands.[17]

Received: June 18, 2012
Published: July 23, 2012

dx.doi.org/10.1021/ja305890c | *J. Am. Chem. Soc.* 2012, 134, 12869−12878

The use of hydrogen bonds as control elements in enantioselective reactions has been triggered in our group by the search for noncovalent interactions, which are compatible with photochemical reaction conditions and which can provide a sufficient steric bias for enantioface differentiation.[18] This work led to chiral sensitizer **1** (Figure 1), which was shown to

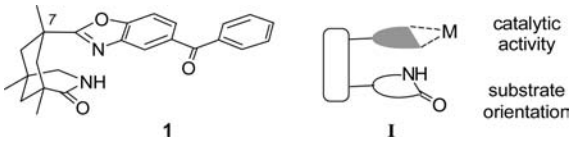

Figure 1. Chiral sensitizer **1** and model for a chiral bifunctional ligand **I** bound to a catalytically active transition metal M (M = metal center, gray = ligand).

provide moderate to good enantioselectivity in a photoinduced electron transfer (PET) reaction.[19] A related sensitizer, which is also based on the rigid 1,5,7-trimethyl-3-azabicyclo[3.3.1]-nonan-2-one skeleton, delivered high enantioselectivities in the intramolecular [2 + 2]-photocycloaddition of certain 4-alkenyl substituted quinolones.[20] Since the bicyclic lactam skeleton has been shown to bind to a variety of amides and lactams,[18,21] it was conceived that chiral bifunctional ligands of type **I** could prove to be useful in enantioselective transition metal catalysis.

Despite the similarity in design, the mode of action of a thermal metal-catalyzed vs a photochemical sensitizer-catalyzed reaction is distinctly different. In the former case the orientation and distance between the reacting substrate and the transition metal are crucial for regio- and enantiocontrol, while in the latter case the sensitizing unit serves only as a steric shield and hardly influences the regioselectivity of the reaction. In order to provide high flexibility regarding potential metals and regarding potential binding modes, a modular approach for the construction of compounds **I** (Figure 1) was developed, in which the metal binding part (in gray) could be installed by Sonogashira cross-coupling[22] or [3 + 2]-cycloaddition[23] to an alkyne. Compounds with the general structure **II** (Figure 2) are

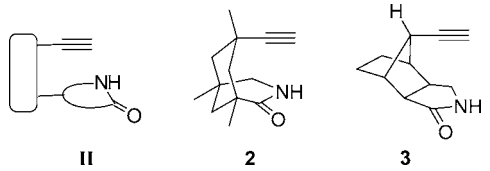

Figure 2. Alkyne templates with a lactam binding site in a general representation **II** and in more specific examples **2** and **3**.

represented by the specific lactams **2**[24] with a 1,5,7-trimethyl-3-azabicyclo[3.3.1]nonan-2-one skeleton[25] and **3**[26] with an octahydro-1*H*-4,7-methanoisoindol-1-one skeleton.[27] Both compounds are available in enantiomerically pure form based on known procedures either from Kemp's triacid[28] or from the Diels–Alder product of 6,6-dimethylfulvene and maleic anhydride.[29]

In preliminary work[26] it was shown that the ruthenium porphyrin complex **4** (Figure 3) can be easily prepared by the Sonogashira cross-coupling reaction[22,30] of alkyne **3** with the respective monobromo-substituted ruthenium porphyrin,[31] which was in turn prepared[32] from the known monobromo-porphyrin[33] (see Supporting Information). In addition, the *N*-methylated compound **5** and an achiral analogue **6** of

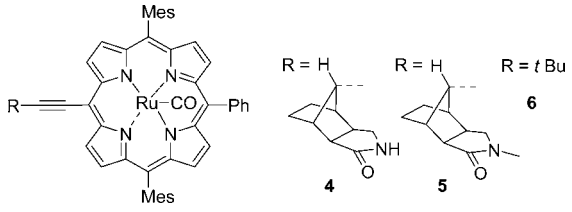

Figure 3. Structure of ruthenium porphyrin complexes **4**–**6**, obtained by Sonogashira cross-coupling reactions.

compound **4** were synthesized. Compound **4** exhibited excellent catalytic properties in the enantioselective epoxidation[34] of 3-vinylquinolone (95% *ee* with a 1 mol % catalyst loading), and by comparison to catalyst **5**, it could be shown that the enantioselectivity is due to the presence of *two* hydrogen bonds between the quinolone and the lactam. The absolute configuration of the resulting epoxide was proven, and a model was suggested to explain the observed selectivity. Moreover, it was shown with 3,7-divinylquinolone that the epoxidation proceeded with higher regioselectivity than the reaction, which was catalyzed by catalyst **6**. We have now collected further data, which substantiates that the enantioselective epoxidiation is generally applicable to 3-alkenylquinolones (10 examples, 86–98% *ee*). The required starting materials were synthesized, and their epoxidation reactions were studied. Previous calculations, which had been conducted on a semiempirical level, have been refined. The DFT calculations now performed show in detail the approach of the electrophilic Ru-complex to the substrate and confirm the observed enantioface differentiation. Amides and pyridones with a suitable olefinic double bond were tested as substrates in the epoxidation reactions, providing significant enantioselectivities (70–87% *ee*) and confirming the stereospecifity (*syn* addition) of the epoxidation reaction. Full details of our work are presented in the following sections of this paper.

RESULTS AND DISCUSSION

Enantioselective Epoxidation of 3-Alkenylquinolones.

Previous epoxidation studies had only been performed with literature known 3-vinylquinolone (**7a**,[35] Figure 4) as the

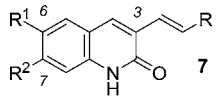

	7a	7b	7c	7d	7e	7f	7g	7h	7i	7j	7k
R	H	Me	Et	^{i}Pr	H	H	H	H	H	H	H
R^1	H	H	H	H	MeO	MeO_2C	Me	H	H	H	H
R^2	H	H	H	H	H	H	H	MeO	MeO_2C	Me	F

Figure 4. Structure of 3-alkenylquinolones **7** employed in this study.

substrate.[26] In order to further evaluate the reaction scope several other substituted 3-alkenylquinolones (Figure 4) were prepared. A substitution at position C6 or C7 seemed useful to investigate the electronic influence on the *para*-positioned nitrogen atom (C6) or the *para*-positioned α,β-unsaturated double bond (C7).

All quinolones **7**, with the exception of **7a**, have not yet been reported in the literature. Two routes were employed to access this compound class. If the corresponding 3-formylquinolone was known, it was attempted to perform the olefination by a

dx.doi.org/10.1021/ja305890c | J. Am. Chem. Soc. 2012, 134, 12869–12878

Wittig reaction.[36] Unsubstituted 3-formylquinolone (**8**),[37] for example, could be converted into the *E*-configured olefin **7b** by treatment with the respective phosphorus ylide (Scheme 1).

Scheme 1

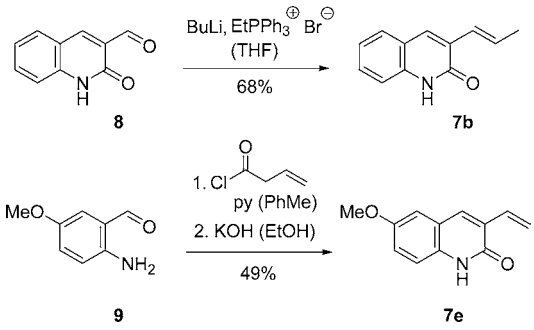

The *Z*-olefin was observed as a byproduct but could not be isolated in pure form. Attempts to obtain the *Z*-isomer of compound **7b** by Suzuki cross-coupling of 3-bromoquinolone were more successful. The compound isomerized readily, however, even in the solid state, which prevented its use in the epoxidation reaction. The 3-alkenylquinolones **7c**, **7g**, and **7j** were also obtained by Wittig reaction of the respective aldehydes (for more details, see the Supporting Information).

An alternative approach was chosen if the corresponding *ortho*-amino- or *ortho*-nitrobenzaldehydes were known or commercially available. In this case, *N*-acylation, for the nitro compounds after a preceding reduction, with the acid chloride of a β,γ-unsaturated acid, led to an immediate precursor for an intramolecular aldol condensation, which was performed with KOH in ethanol.[35] As an example the reaction of *ortho*-aminobenzaldehyde **9**[38] with 3-butenoyl chloride is shown in Scheme 1, which led to 3-vinylquinolone **7e** in a two-step sequence. In an analogous fashion the quinolones **7d**, **7f**, **7h**, **7i**, and **7k** were synthesized (for more details, see the Supporting Information).

Quinolones **7** could be oxidized to the respective racemic epoxides *rac*-**10** with *meta*-chloroperbenzoic acid (*m*CPBA) in dichloromethane. All products could be readily isolated except for the epoxide derived from quinolone **7h**, which was unstable and underwent unspecific ring-opening reactions. The enantioselective epoxidation was initially performed with 1 mol % of catalyst **4**, but it was found that in most cases 0.2 mol % of the catalyst was sufficient to obtain optimal results (Scheme 2). 2,6-Dichloropyridine-*N*-oxide was used as a stoichiometric oxidant,[39] which was, together with the substrate (c = 20 mM), dissolved in benzene at ambient temperature. The catalyst was added as a benzene solution, and the reaction mixture was stirred for 24 h before workup. The results of these experiments are summarized in Table 1.

Scheme 2

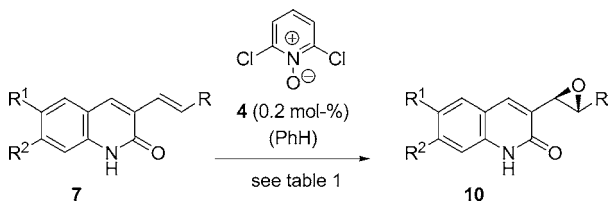

Most substrates reacted cleanly in good yields with high enantiomeric excess (85−98% *ee*). A modification of the R substituent at the vinylic double bond from hydrogen (entry 1) to alkyl (entries 2−4) resulted in slighly lower enantiomeric excesses (86−88% *ee*). The isopropyl-substituted substrate **7d** (entry 4) exhibited a diminished chemoselectivity despite the fact that conversion was complete after 24 h. Substitution at carbon atom C6 turned out to be beneficial for the enantioselectivity (entries 5−7), and substrates **7e**−**7g** gave the highest enantioselectivity (95−98% *ee*) of all the quinolones. Ester **7f** (entry 6) and ester **7i** (entry 9) showed only a reduced solubility in benzene, and they were consequently employed in a concentration of 10 mM. Still, the reactions remained incomplete, and unreacted starting material was recovered after 24 h. Methoxy substitution at carbon atom C7 (entry 8) was detrimental for the reactivity and for the product stability. In line with the insufficient chemoselectivity observed in its epoxidation by *m*CPBA (vide supra), the Ru-catalyzed epoxidation of substrate **7h** was sluggish and the resulting epoxide could not be isolated in pure form. The reaction did not go to completion, and in the crude product mixture the substrate was detected in significant amounts (product/substrate = 64/36 by ^{1}H NMR integration) even after a reaction time of 48 h. The other substituents R^2 (entries 8−11) had, apart from the reduced solubility of **7i**, little influence on the reactivity when compared to the parent 3-vinylquinolone (**7a**). The corresponding epoxides **10i**−**k** were produced in good yields and with high enantioselectivity (85−92% *ee*). All yields were diminished by the instability of the epoxides on silica gel or on alumina. Rearrangement products were observed in some cases, explaining in part why the yields of the isolated product generally did not exceed 80% despite the fact that the epoxidation reactions proceeded cleanly and without a significant byproduct. Compounds of type **10** have previously not been accessible in an enantioselective fashion.[40]

The absolute product configuration of epoxides **10** was assigned based on the previously established configuration of epoxide **10a**.[26] The assignment was confirmed by further studies (vide infra) and by the fact that all epoxides **10** were consistently levorotatory. The reaction proceeded diastereoselectively for *E*-configured olefins **7b**−**7d**, and only the *trans*-configured epoxides **10b**−**10d** were isolated. Since the *Z*-configured olefins could not be obtained in pure form, it was not possible to prove the stereospecifity of the epoxidation for 3-alkenylquinolones **7**. However, it was shown that *Z*-configured olefins do undergo the enantioselective epoxidation. The tricyclic substrate **13** for example was readily available by ring closing metathesis[41] from 4-(3-butenyl)-3-vinylquinolone (**12**), which in turn was accessible in three steps from *ortho*-aminobenzonitrile (**11**). Due to its insufficient solubility in benzene, substrate **13** was epoxidized in dichloromethane (Scheme 3). The reaction proceeded slowly at a substrate concentration of 5 mM, but it delivered epoxide **14** with an excellent enantioselectivity of 92% *ee*. The reaction was complete after 48 h, and the product was isolated in 62% yield.

The crucial influence of the hydrogen bonding between the substrate and catalyst **4** was demonstrated by a competition experiment with quinolone **7a** and its *N*-methylated derivative **15** (Scheme 4). After 4 h the product ratio **10a**/**16** was 91/9, and after 24 h it changed slightly to 84/16. The conversion was almost complete (93% conversion) for substrate **7a** after 24 h, and product **10a** was isolated in 74% yield. In an independent experiment, the oxidation of substrate **15** was performed under

dx.doi.org/10.1021/ja305890c | J. Am. Chem. Soc. 2012, 134, 12869−12878

Table 1. Reaction Conditions, Yields, and Enantioselectivities in the Ru-Catalyzed Epoxidation of Quinolones 7 (see Scheme 2)

entry	substrate[a]	R	R^1	R^2	product	yield[b] [%]	ee[c] [%]
1	**7a**	H	H	H	**10a**	72	96
2	**7b**	Me	H	H	**10b**	74	86
3	**7c**	Et	H	H	**10c**	83	86
4	**7d**	^{i}Pr	H	H	**10d**	60	87
5	**7e**	H	MeO	H	**10e**	69	98
6	**7f**[d]	H	MeO_2C	H	**10f**	49(71)[e]	96
7	**7g**	H	Me	H	**10g**	70	95
8	**7h**	H	H	MeO	**10h**	——[f]	——
9	**7i**[d]	H	H	MeO_2C	**10i**	45(70)[e]	85
10	**7j**	H	H	Me	**10j**	65	92
11	**7k**	H	H	F	**10k**	71	92

[a]The reactions were conducted at a substrate concentration of 20 mM at ambient temperature in benzene as the solvent, employing 1.1 equiv of 2,6-dichloropyridine-*N*-oxide as the oxidant and 0.2 mol % catalyst **4**. The reaction time was 24 h. [b]Yield of isolated product. [c]The enantiomeric excess was determined by chiral HPLC (see Supporting Information). [d]Due to the low solubility of the substrate the reaction was performed at a substrate concentration of 10 mM. [e]The reaction remained incomplete after 24 h. The yield in brackets is based on recovered starting material. [f]The product was formed sluggishly and could not be isolated (see narrative for more information).

Scheme 3

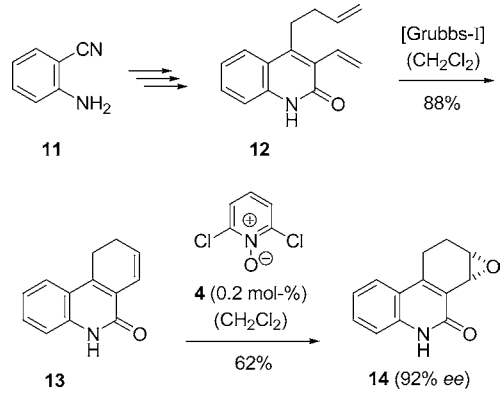

Scheme 4

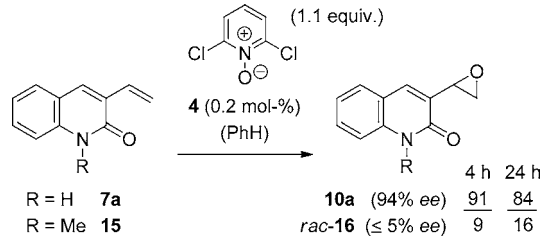

the typical conditions for quinolone oxidation with 0.2 mol % catalyst. It was found that the reaction was close to completion after 24 h and yielded product *rac*-**16** in 62% yield without any detectable *ee* (≤5% *ee*). Similarly, the *N*-methylated derivative **5** of catalyst **4** (Figure 3) induced only a low enantioselectivity (14% *ee*) in the epoxidation of 3-vinylquinolone (**7a**).[26]

DFT Calculations and Mode of Action. Although the studies with the *N*-methylated derivatives just described clearly indicate that there is a two-point hydrogen bond interaction between the lactam part of catalyst **4** and the quinolone amide function at nitrogen atom N1 and carbon atom C2, the exact mode of the oxygen transfer from the ruthenium porphyrin complex and the enantioface differentiation was further investigated. Seminal studies by Groves et al. in the 1980s had been performed with dioxo(tetramesitylporphyrinato)-ruthenium(VI), which was shown to be competent for stoichiometric olefin epoxidation under anaerobic conditions and for catalytic olefin epoxidation under aerobic conditions.[42] The use of chiral ruthenium porphyrins for enantioselective epoxidation reactions began to be explored in the 1990s,[43] and the enantioselective epoxidation with chiral metalloporphyrin catalysts has remained an active research area to date.[44]

In most racemic and enantioselective Ru-catalyzed epoxidation reactions a dioxo ruthenium(VI) intermediate has been assumed to be the catalytically active intermediate, from which the oxygen transfer to the olefinic double bond occurs.[44] The other oxo substituent serves as a spectator ligand, which remains attached to the ruthenium metal in the monooxo ruthenium(IV) complex, which is subsequently reoxidized to the dioxo species. In our case, the corresponding dioxo complex **17** was expected to deliver the oxygen atom to the epoxide within a hydrogen-bound complex **17**·**7a** (Figure 5). Enantioface differentiation would be possible if the rotation around the carbon−carbon bond, which connects the vinyl group to the quinolone, was restricted.

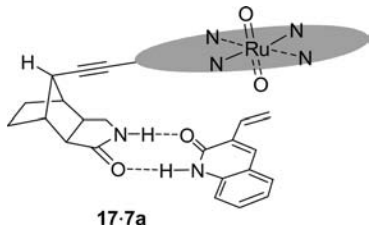

Figure 5. Preliminary model of the oxygen transfer from the reactive Ru-complex **17** derived from complex **4** to 3-vinylquinolone (**7a**) (the porphyrin skeleton is schematically drawn in gray).

As illustrated by Scheme 5, an s-*cis*-configured 3-alkenylquinolone would require an *Si* face attack (relative to

Scheme 5

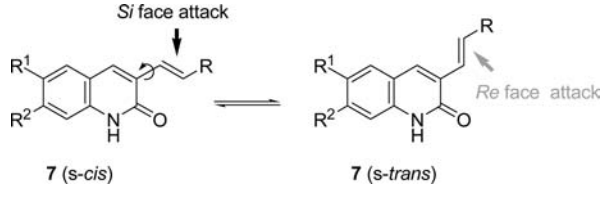

dx.doi.org/10.1021/ja305890c | J. Am. Chem. Soc. 2012, 134, 12869−12878

the *internal* prostereogenic carbon atom of the double bond) of the oxygen atom to account for the enantioselective formation of products **10**, while in the complex depicted in Figure 5, the Re face of the s-*trans*-conformer was to be attacked. In order to confirm that there is a significant difference in the transition states leading from quinolones **7** to products **10**, theoretical calculations were performed, in which 3-vinylquinolone (**7a**) served as a representative olefin.

For the DFT investigations, the M06L[45] density functional was used in combination with the Stuttgart/Dresden[46] basis set (including the corresponding pseudopotential) for ruthenium and the 6-31G(d)[47] basis set for all other atoms. All calculations were performed on the untruncated complexes, using Gaussian09[48] with the grid=ultrafine option for integral evaluation. Since the initial attack of the Ru-bound oxo substituent on the vinyl group of the substrate is clearly the selectivity-determining step, we focused our calculations on the transition states of this process. The nature of these transition states was verified by analytic computation of vibrational frequencies: all structures reported below show one imaginary frequency corresponding to the above-mentioned attack of an oxo substituent on the quinolone substrate.

Calculations were initially performed on both the singlet and the triplet energy surface. No spin contamination was found for the (unrestricted) singlet structures, validating the treatment of these systems with the single-reference DFT methodology. The triplet transition states of the dioxo complex **17** with both **7a** (s-*cis*) and **7a** (s-*trans*) turned out to be approximately 58 kJ/mol higher in free energy than their respective singlet equivalents and were as a consequence not considered to be relevant in the context of this investigation.

On the singlet energy surface, the transition state of **17**·**7a** with the substrate in the s-*trans* conformation, $\mathbf{TS}_{trans}$ (Figure 6), was found to be more stable than the transition state with

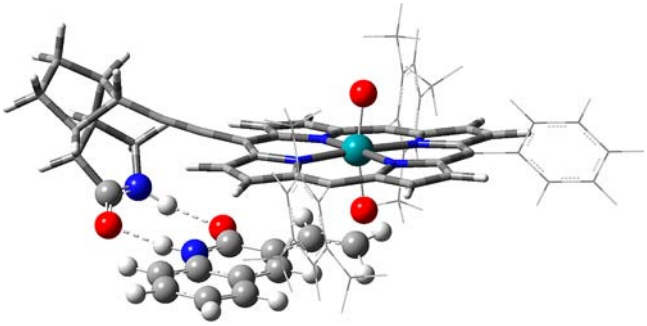

Figure 6. Transition state $\mathbf{TS}_{trans}$ for the attack of an oxo substituent of **17** on the vinyl group of quinolone **7a** in an s-*trans* conformation. The substrate is bound to the Ru complex by a two-point hydrogen bond. For better comprehensibility, various parts of the Ru complex are shown with different visualization styles, although all parts of the complex have been treated equivalently.

the substrate in the s-*cis* conformation, $\mathbf{TS}_{cis}$ (Figure 7), by 21 kJ/mol in energy (or 12 kJ/mol in free energy). This difference in energy thus provides a rationalization of the experimental results mentioned above, as the more favorable transition state features an *Re* face attack on the s-*trans* conformer of the substrate, leading to the experimentally found enantioselectivity.

In both cases, the oxo substituent attacks the terminal carbon atom of the vinyl group. The corresponding O−C distances are

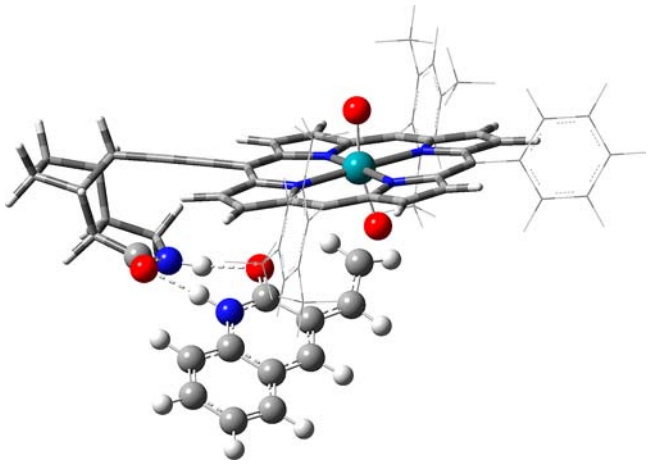

Figure 7. Transition state $\mathbf{TS}_{cis}$ for the attack of an oxo substituent of **17** on the vinyl group of quinolone **7a** in an s-*cis* conformation. The substrate is bound to the Ru complex by a two-point hydrogen bond. For better comprehensibility, various parts of the Ru complex are shown with different visualization styles, although all parts of the complex have been treated equivalently.

1.85 Å for the favorable $\mathbf{TS}_{trans}$ and 1.80 Å for the less favorable $\mathbf{TS}_{cis}$ transition state. The Ru−O bond on the site of the attack is somewhat elongated, with a bond length of 1.83 Å for $\mathbf{TS}_{trans}$ and 1.84 Å for $\mathbf{TS}_{cis}$, compared to 1.75 Å for the Ru−O bond on the site opposite to the attack. The same is true for the C=C bond length of the vinyl subunit, which equals 1.39 Å for $\mathbf{TS}_{trans}$ and 1.40 Å for $\mathbf{TS}_{cis}$ (compared to 1.34 Å for the isolated substrate in both the s-*trans* and s-*cis* conformation). In both transition states, there is only a very weak, if any, interaction of the oxo substituent with the inner carbon atom of the vinyl group. The respective O−C distances are 2.61 Å for $\mathbf{TS}_{trans}$ and 2.53 Å for $\mathbf{TS}_{cis}$. As expected, the terminal carbon atom is partly pyramidalized, while the inner carbon atom remains planar.

The most obvious structural differences between the two transition states concern the binding of the substrate to the ligand and, to a lesser extent, the deformation of the C−C triple bond that links the porphyrin core to the chiral hydrogen bond template of the ligand. In the more favorable $\mathbf{TS}_{trans}$, the plane of the quinolone ring is essentially parallel to the plane of the porphyrin ring. In order to accomplish this, the substrate does not occupy the plane formed by the hydrogen bond motif of the chiral ligand, but is bent toward the porphyrin with an angle of approximately 40°. The C—C triple bond of the ligand shows some deviation from a linear arrangement, with C—C≡C and C≡C—$C_{porphyrin}$ angles of 172° and 175°, respectively. As a consequence, the torsion angle of the vinyl group of the substrate with respect to the quinolone ring is only 6° in the transition state.

In the less favorable $\mathbf{TS}_{cis}$, the quinolone ring is not parallel to the porphyrin ring or to the hydrogen bond binding motif of the ligand, but features a slight rotation around an axis equivalent to the hydrogen bonding direction. The C—C triple bond of the ligand is markedly more linear (with C—C≡C and C≡C—$C_{porphyrin}$ angles of 178° and 179°, respectively). The torsion of the vinyl group of the substrate with respect to the quinolone ring is increased in this case and equals 17°. The different torsion angles of the vinyl group in the two transition states seem to indicate that more energy is required to distort the substrate from the ground state geometry to the geometry found in the transition state in the case of the less favorable

dx.doi.org/10.1021/ja305890c | J. Am. Chem. Soc. 2012, 134, 12869−12878

transition state. This might explain at least part of the energetic difference between both cases. In order to verify this assumption computationally, we calculated the respective energies required to distort **7a** from its equilibrium geometry to the geometry of the isolated substrate in the transition state for both the s-*trans* and the s-*cis* conformer.[49] We found, however, little difference in these deformation energies (34 kJ/mol for s-*trans* and 37 kJ/mol for s-*cis*). While this type of analysis certainly has only orientating character, it seems to indicate that the stronger deformation of the substrate in the case of $\mathbf{TS}_{cis}$ is *not* the deciding factor for the energetic differences in both transition states. The same analysis for the ruthenium porphyrin complex, however, yielded deformation energies of 26 kJ/mol for $\mathbf{TS}_{trans}$ and 41 kJ/mol for $\mathbf{TS}_{cis}$, and thus a much larger difference between the two terms. The distortion of the ruthenium complex consequently seems to be one important component, which is responsible for the energy difference of the two transition states.

A second component, which contributes to the energetic difference between $\mathbf{TS}_{trans}$ and $\mathbf{TS}_{cis}$, is due to a disparity between the binding strengths of the two-point hydrogen bond motifs. While the exact interaction energy is somewhat difficult to assess considering the rather moderate basis sets employed, we observed a difference in the interaction distances for both structures. Thus, while the $NH_{ligand}-O_{substrate}$ distance is essentially the same for both cases (1.86 Å for $\mathbf{TS}_{trans}$ and 1.85 Å for $\mathbf{TS}_{cis}$), the $O_{ligand}-HN_{substrate}$ distance is somewhat longer for $\mathbf{TS}_{cis}$ (1.81 vs 1.77 Å), indicating a weaker hydrogen bond. It seems that, for $\mathbf{TS}_{cis}$, the slight rotation of the quinolone ring around the hydrogen-bonding axis, while necessary to bring the s-*cis* vinyl group close enough to the oxo substituent, also reduces the binding strength of the substrate to the ligand. All issues considered, less deformation of the binding partners is needed to reach $\mathbf{TS}_{trans}$, and this, together with the (presumably) stronger hydrogen-bond interaction energy, serves to explain why this transition state is more stable and why, experimentally, the enantiomer corresponding to an *Re* attack on the s-*trans* substrate is found as the product.

It was probed computationally whether any influence of the quinolone substitution pattern can be detected. More specifically, the transtition states for the reactions of substrates **7f** and **7i** were calculated (for details, see Supporting Information). Most importantly, for both **7f** and **7i**, again a preference for $\mathbf{TS}_{trans}$ was found by the DFT calculations. The energetic difference between $\mathbf{TS}_{trans}$ and $\mathbf{TS}_{cis}$ was almost identical to the one found for **7a** in the case of substrate **7f** (approximately 12 kJ/mol) and slightly higher for substrate **7i** (approximately 16 kJ/mol). The large size of the investigated system prevented the use of more accurate computational methods. The calculated energetic differences are not considered sufficiently precise to account for the minor differences in the experimentally observed enantioselectivities.

Mechanistic Discussion. Based on previous reports about Ru-catalyzed oxidation reactions,[39,43,44] on our own experience in the field of hydrogen bond mediated enantioselective reactions,[18−21] and on the calculations discussed in the preceding paragraph, a mechanistic pathway can be proposed, which is depicted in Scheme 6 with quinolone **7a** as a representative substrate.

A ruthenium(VI) complex **17** is suggested as the reactive species, which is formed from compound **4** by oxidation with 2,6-dichloropyridine-*N*-oxide. An approach of the substrate

Scheme 6

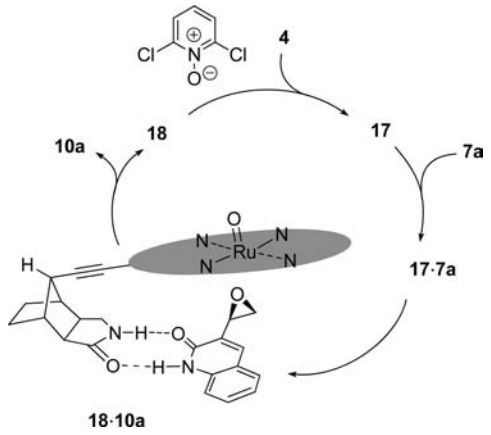

leads to formation of the binary complex **17·7a** (Figure 5), in which oxygen transfer via transition state $\mathbf{TS}_{trans}$ (Figure 6) is rapid. Based on association[21b] and kinetic[20b] data obtained for related hydrogen bound complexes, the rate for the dissociation of complex **17·7a** can be estimated to be on the order of 10^7 s^{-1} at ambient temperature. The question of whether oxygen transfer is faster than dissociation, i.e. whether complex formation is reversible, cannot be answered at this point in time. In any case, the transition state $\mathbf{TS}_{trans}$, which leads to the oxidized product in complex **18·10a**, is energetically favored over any transition state, which operates without hydrogen bonding interactions (see Scheme 4). Formation of the enantiomeric product *ent*-**10a** could be explained by population of $\mathbf{TS}_{cis}$, which is higher in energy. However, competing transition states in the selectivity-determining step, which proceed via no or single-point hydrogen bonding, are also accessible. For the reaction of *N*-vinylquinolones **7a**, **7e−7g**, **7i−7k** it appears as if the binding properties are responsible for the different enantioselectivities observed; i.e. unselective reactions proceed via competing transition states without a clear directivity. Indeed, the calculations show no significant energy differences for the two doubly hydrogen-bound transitions states irrespective of methoxycarbonyl substitution in the 6- or 7-position (vide supra). Contrary to that, the binding properties of *N*-alkenylquinolones **7a−7d** should be identical and it is likely that formation of the minor enantiomers occurs in these cases via diastereomorphic transition states related to the s-*cis* rotamers of the respective substrate (Scheme 5). Subsequent dissociation of the product enables reoxidation of ruthenium(IV) complex **18** to the catalytically active species **17**.

The instability of the product epoxides **10** made quantitative kinetic analysis of the epoxidation reaction difficult. In addition, an induction period was observed in the reactions, presumably due to the fact that compound **4** is initially oxidized to the catalytically active species. This process is not necessarily quantitative. In other words, a direct correlation between the amount of compound **4** and the formation of the putative catalytically active species **17** does not exist. Lowering the amount of catalyst **4** to 0.1 mol % under otherwise identical conditions still led to an almost complete conversion (94%) after 24 h, and product **10a** was isolated in 67% yield. At a catalyst concentration of 0.05 and 0.01 mol %, the reaction remained incomplete. Product **10a** was isolated together with the starting material. Product yields were 65% for 0.05 mol % and 47% for 0.01 mol %. The enantiomeric excess of the

dx.doi.org/10.1021/ja305890c | J. Am. Chem. Soc. 2012, 134, 12869−12878

product remained, within the limits of error (±1% *ee*), unchanged at a catalyst concentration of ≥0.05 mol % showing the high stereochemical fidelity of the catalyst even at low concentration. Only at very low catalyst loading (0.01 mol %) did the enantioselectivity decrease to 92% *ee*. Turnover numbers are high. Given that 0.01 mol % of the catalyst facilitates a substrate conversion of close to 50% after 24 h, the turnover number exceeds 4000.

Additional qualitative data were obtained from reactions, which were interrupted after a reaction time of 4 h (Table 2).

Table 2. Influence of Different Conditions on the Ru-Catalyzed Epoxidation of 3-Vinylquinolone (7a) after 4 h

entry	catalyst[a]	equiv oxid.[b]	additive	**10a**/**7a**[c]	yield[d] [%]	*ee*[e] [%]
1	**4**	1.1	—	50/50	37	96
2	**4**	0.55	—	23/77	14	93
3	**4**	2.2	—	79/21	57	96
4	**4**	1.1	3-EQ[f]	53/47	39	93
5	**6**	1.1	—	19/81	15	—

[a]The reactions were conducted at a substrate concentration of 20 mM at ambient temperature in benzene as the solvent, employing 2,6-dichloropyridine-*N*-oxide as the oxidant and 0.2 mol % catalyst. The reaction time was 4 h. [b]Equivalents of 2,6-dichloropyridine-*N*-oxide employed in the reaction. [c]The ratio of product/substrate was determined by ^{1}H NMR integration. [d]Yield of isolated product. [e]The enantiomeric excess was determined by chiral HPLC. [f]The reaction was performed in the presence of stoichiometric amounts (1 equiv) of 3-ethylquinolone (3-EQ).

The initial reaction rate depends significantly on the amount of oxidant being used in the process (entries 1−3). After 4 h and with 1.1 equiv of 2,6-dichloropyridine-*N*-oxide the conversion of substrate **7a** was complete to a degree of roughly 50% (product/substrate = 50/50) in the presence of 0.2 mol % of catalyst **4**. With 0.55 equiv of the oxidant the conversion dropped to 23% (entry 2) and it increased to 79% with 2.2 equiv of the oxidant (entry 3). The data suggest that the oxidant is involved in the rate-determining step, which appears to be the oxidation of ruthenium(IV) complex **18** to the ruthenium(VI) complex **17**.

The fact that the epoxidation step (**17**·**7a** → **18**·**10a**) is not rate determining is further supported by the fact that the catalytic performance was not influenced by the addition of another 3-substituted quinolone, which competes with the binding site. 3-Ethylquinolone (3-EQ) was added in stoichiometric amounts to the catalytic epoxidation **7a** → **10a**, and the reaction was stopped after 4 h (entry 4). The product/substrate ratio was identical (product/substrate = 53/47) as compared to the reaction without an additive (entry 1). The enantiomeric excess was slightly lower (93% *ee*). The rate but not the enantioselectivity was influenced at higher 3-EQ concentrations. After 10 h and with 5 equiv of 3-EQ (see Supporting Information), the product/substrate ratio decreased from 43/57 (no additive) to 21/79 and, with 10 equiv, to 15/85. There was only a minor deviation in the enantiomeric excess (92% and 91% *ee*). These data suggest that reoxidation can only occur when the binding site is vacant. Blocking the binding site retards the reoxidation of **18** to **17**. Regarding the reoxidation from Ru(IV) to Ru(VI), the situation for catalyst **6** is likely to be different because the ruthenium center is much easier to approach by the oxidant. The lower conversion in this case (entry 5) can be explained by a slower epoxidation reaction as compared to the rapid epoxidation within complex **17**·**7a**.

Enantioselective Epoxidation of Other Substrates. From the picture of the preferred transition state $\mathbf{TS}_{trans}$ of the epoxidation reaction, it is evident that any substrate in which the double bond in the 3-position of the quinolone cannot readily adopt an s-*trans* conformation will be difficult to oxidize. Indeed, the previously mentioned compound **12** (Figure 8), which bears a butenyl group at C4, failed to react

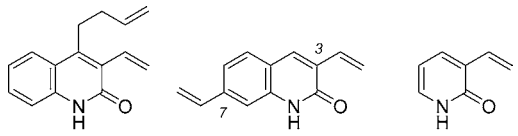

12 **19** **20a**

Figure 8. Structures of 3-vinyl-substituted quinolones **12**, **19**, and pyridone **20a**.

cleanly under the typical reaction conditions, which were applied to substrates **7**. In addition, the reaction was by far less enantioselective. The respective epoxide was obtained in a yield of 39% after a reaction time of 24 h and with 31% *ee*.

The highly ordererd transition state of the epoxidation reaction also suggests that the epoxidation occurs with high regioselectivity if a substrate contains two electronically similar vinylic double bonds. Compound **19** for example was shown to undergo the epoxidation with catalyst **4** in a regioselectivity of 91/9 in favor of the double bond in the 3-position (88% *ee*).[26] Under the same reaction conditions, the use of catalyst **6** led to a sluggish conversion, which was not complete even after 40 h and which resulted in a regioisomeric ratio of 62/38.

Given the lactam binding mode operating in the case of quinolones **7**, it was expected that the analogous 3-alkenylpyridones would react with similar enantioselectivity as the respective quinolones. It must be noted, however, that epoxides of 3-alkenylpyridones have to the best of our knowledge not yet been described in the literature. It was consequently not unexpected that the parent 3-vinylpyridone (**20a**)[50] delivered an epoxide, which was impossible to isolate by column chromatography on silica or on alumina. In addition, like in the case of substrate **7h**, the reaction proceeded slowly and with low chemoselectivity. The 5-substituted pyridones **20b**[51] and **20c**[52] reacted more efficiently, but the isolation problems persisted. Despite the fact that the reaction was complete after 24 h, the epoxides could not be purified and determination of the *ee* was not possible. Eventually the intermediate epoxides were opened with a sulfur nucleophile (*para*-thiocresol, ArSH),[53] and the enantiomeric purity of the resulting secondary alcohols was determined (Scheme 7). The enantioselectivity was high in both cases, and the analogy to the quinolone examples seems to hold.

Scheme 7

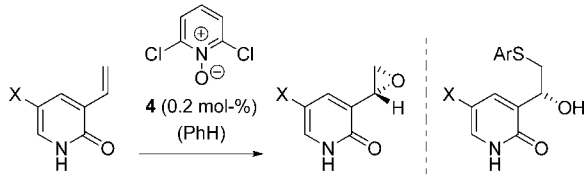

20b X = CF_3 **21b** (87% *ee*)
20c X = CO_2Me **21c** (77% *ee*)

dx.doi.org/10.1021/ja305890c | *J. Am. Chem. Soc.* 2012, 134, 12869−12878

While both quinolones and pyridones display a lactam binding site, it seemed appropriate to investigate whether primary alkenoic amides would also be amenable to an enantioselective epoxidation reaction. Literature known amide **22**[54] was prepared and subjected to the standard reaction conditions (Table 1) employing, however, 1.5 mol% of catalyst **4**. The higher catalyst loading was required to enforce a complete reaction after three days. The reaction yielded 61% of *cis*-epoxide **23** in 70% *ee* (Scheme 8). For this example the

Scheme 8

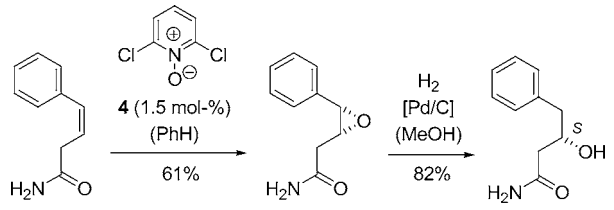

stereospecifity of the epoxidation process could be proven because the *trans*-alkenoic amide was also synthetically accessible.[55] It has been previously observed that *trans*-substituted styrenes are less reactive in Ru-catalyzed epoxidation reactions.[39b] In line with this observation, conversion of the *trans*-substrate was very slow (16% conversion after four days), and product formation remained incomplete. However, the only detectable product was the *trans*-epoxide.

The absolute configuration of epoxide **23** was established upon hydrogenolysis to the secondary alcohol **24**, which could be independently obtained from enantiomerically pure (*S*)-methyl phenyllactate (see Supporting Information). The stereochemical identity of the compounds was proven by chiral HPLC and chiroptical methods (specific rotation). The outcome of this reaction supports the model for oxygen transfer in the hydrogen-bound complex (Figure 5). Amide **22** is able to adopt a conformation similar to quinolones **7** and exposes the double bond to the ruthenium(VI) dioxo complex **17** in the same fashion as the respective s-*trans* conformers of **7**. The lower selectivity is likely due to the higher degree of rotational freedom. While there is only one single bond in quinolones **7**, around which a rotation is possible, amide **22** contains two single bonds between the amide group and the reactive double bond. The situation becomes even more complicated for carbamate **25**[56] (Scheme 9), in which there are three single bonds between the binding motif and the reacting center. In this case, the enantioselectivity of the epoxidation further decreased and product **26** was obtained in a good yield of 69% but with only moderate enantioselectivity (45% *ee*).

Scheme 9

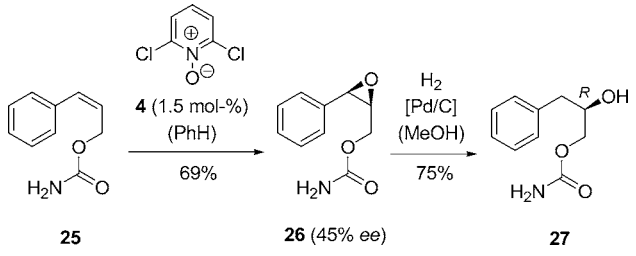

Proof of the absolute configuration was obtained for compound **26** again by hydrogenolysis to a secondary alcohol. The resulting product **27** could be obtained also from (*S*)-methyl phenyllactate (see Supporting Information). In this case, however, the synthetic product showed the opposite absolute configuration and the (*R*)-configuration was consequently assigned to the stereogenic center in compound **27**. Apparently carbamate **25** prefers a stretched conformation in the reactive complex (Figure 9) avoiding 1,3-allylic strain between the phenyl group and the oxygen atom.

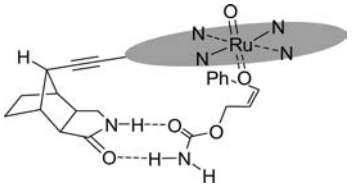

Figure 9. Model for the oxygen transfer to the olefinic double bond in primary amide **25** (the porphyrin skeleton is schematically drawn in gray).

The last two results show that primary amides can be used in enantioselective reactions, in which the enantioselectivity is transferred from a rigid chiral backbone to the reaction center via hydrogen bonds. However, the higher conformational flexibility of these substrates is detrimental to the required enantioface differentiation.

CONCLUSION

The present study provides convincing evidence that the presence of two hydrogen bonding sites at a chiral bifunctional ligand allows for highly enantioselective reactions, which occur at a spatially remote metal center. Substrate coordination via hydrogen bonding lowers the transition state of the metal catalyzed process so that it occurs almost exclusively within the hydrogen-bound complex. The chiral information is transmitted via the chiral ligand backbone over a distance of more than 7.0 Å. The general binding mode enables a substrate variation as long as the reactive center is exposed to the catalytically active metal in a defined fashion. Although the current study is the first of its kind and has limited predictive character, further optimization should lead to supramolecular catalysts, which are able to attack less activated reactive centers than double bonds. In addition it should be possible to change the regioselectivity of attack by shortening or lengthening the distance between the hydrogen bonding site and the catalytically active center. Work along these lines continues in our laboratories.

ASSOCIATED CONTENT

Supporting Information

Detailed experimental procedures, characterization data for new compounds, and details of the DFT calculations. This material is available free of charge via the Internet at http://pubs.acs.org.

AUTHOR INFORMATION

Corresponding Author

thorsten.bach@ch.tum.de

Notes

The authors declare no competing financial interest.

■ ACKNOWLEDGMENTS

This project was supported by the *Deutsche Forschungsgemeinschaft* (Ba 1372-17) and by the *TUM Graduate School*. We thank Wacker-Chemie (Munich) for the donation of chemicals. S.M.H. thanks the *Fonds der Chemischen Industrie* for a Liebig fellowship.

■ REFERENCES

(1) Hartwig, J. F. *Organotransition Metal Chemistry: From Bonding to Catalysis*; University Science: Sausalito, CA, 2010.
(2) van Leeuwen, P. W. N. M. *Supramolecular Catalysis*; Wiley-VCH: Weinheim, 2008.
(3) Review on enzyme mimics based upon supramolecular coordination chemistry: Wiester, M. J.; Ulmann, P. A.; Mirkin, C. A. *Angew. Chem., Int. Ed.* **2011**, *50*, 114−137.
(4) For an excellent recent review, see: Carboni, S.; Gennari, C.; Pignatoro, L.; Piarulli, U. *Dalton Trans.* **2011**, *40*, 4355−4373.
(5) For a short review on scaffolding ligands, see: Tan, K. L.; Sun, X.; Worth, A. D. *Synlett* **2012**, *23*, 321−325.
(6) Review: Crabtree, R. H. *New J. Chem.* **2011**, *35*, 18−23.
(7) Reviews and monographs on cytochrome P450 mimics: (a) Mansuy, D. *Pure Appl. Chem.* **1987**, *59*, 759−770. (b) Mansuy, D. *Pure Appl. Chem.* **1994**, *66*, 737−744. (c) Feiters, M. C.; Rowan, A. E.; Nolte, R. J. M. *Chem. Soc. Rev.* **2000**, *29*, 375−384. (d) Meunier, B. *Biomimetic Oxidations Catalyzed by Transition Metal Complexes*; Imperial College Press: London, 2000. (e) Groves, J. T. *Proc. Natl. Acad. Sci. U.S.A.* **2003**, *100*, 3569−3574. (f) Ortiz de Montellano, P. R. *Cytochrome P450: Structure, Mechanism, and Biochemistry*, 3rd ed.; Kluwer: New York, 2005.
(8) For artificial metalloenzymes, which act by tethering a transition metal to a host protein via hydrogen bonds, see: Ward, T. R. *Acc. Chem. Res.* **2011**, *44*, 47−57.
(9) For the use of hydrogen bonds in organocatalysis, see: Taylor, M. S.; Jacobsen, E. N. *Angew. Chem., Int. Ed.* **2006**, *45*, 1520−1543.
(10) For selective oxidation reactions mediated by other noncovalent interactions except hydrogen bonds, see: (a) Breslow, R.; Zhang, X.; Huang, Y. *J. Am. Chem. Soc.* **1997**, *119*, 4535−4536. (b) Yang, J.; Breslow, R. *Angew. Chem., Int. Ed.* **2000**, *39*, 2692−2694. (c) Yang, J.; Gabriele, B.; Belvedere, S.; Huang, Y.; Breslow, R. *J. Org. Chem.* **2002**, *67*, 5057−5067. (d) Fang, Z; Breslow, R. *Org. Lett.* **2006**, *8*, 251−254.
(11) (a) Grotjahn, D. B.; Miranda-Soto, V.; Kragulj, E. J.; Lev, D. A.; Erdogan, G.; Zeng, X.; Cooksy, A. L. *J. Am. Chem. Soc.* **2008**, *130*, 20−21. (b) Grotjahn, D. B.; Kragulj, E. J.; Zeinalipour-Yazdi, C. D.; Miranda-Soto, V.; Lev, D. A.; Cooksy, A. L. *J. Am. Chem. Soc.* **2008**, *130*, 10860−10861.
(12) (a) Das, S.; Incarvito, C. D.; Crabtree, R. H.; Brudvig, G. W. *Science* **2006**, *312*, 1941−1943. (b) Das, S.; Brudvig, G. W.; Crabtree, R. H. *J. Am. Chem. Soc.* **2008**, *130*, 1628−1637. (c) Hull, J. F.; Sauer, E. L. O.; Incarvito, C. D.; Faller, J. W.; Brudvig, G. W.; Crabtree, R. H. *Inorg. Chem.* **2009**, *48*, 488−495.
(13) (a) Šmejkal, T.; Breit, B. *Angew. Chem., Int. Ed.* **2008**, *47*, 3946−3949. (b) Šmejkal, T.; Gribkov, D.; Geier, J.; Keller, M.; Breit, B. *Chem.—Eur. J.* **2010**, *16*, 2470−2478. (c) Dydio, P.; Dzik, W. I.; Lutz, M.; de Bruin, B.; Reek, J. H. N. *Angew. Chem., Int. Ed.* **2011**, *50*, 396−400.
(14) For additional studies on the directing effect of hydrogen bonds in transition metal catalyzed reactions, see: (a) Coolen, H. K. A. C.; Meuwis, J. A. M.; van Leeuwen, P. W. N. M.; Nolte, R. J. M. *J. Am. Chem. Soc.* **1995**, *117*, 11906−11913. (b) Jónsson, S. S.; Odille, F. G. J.; Norrby, P.-O.; Wärnmark, K. *Chem. Commun.* **2005**, 549−551. (c) Jónsson, S.; Odille, F. G. J.; Norrby, P.-O.; Wärnmark, K. *Org. Biomol. Chem.* **2006**, *4*, 1927−1948. (d) Zhu, S.; Ruppel, J. V.; Lu, H.; Wojtas, L.; Zhang, X. P. *J. Am. Chem. Soc.* **2008**, *130*, 5042−5043. (e) Lu, Y.; Johnstone, T. C.; Arndtsen, B. A. *J. Am. Chem. Soc.* **2009**, *131*, 11284−11285. (f) Dzik, W. I.; Xu, X.; Zhang, X. P.; Reek, J. N. H.; de Bruin, B. *J. Am. Chem. Soc.* **2010**, *132*, 10891−10902 and references cited therein.
(15) Agarkov, A.; Greenfield, S.; Xie, D.; Pawlick, R.; Starkey, G.; Gilbertson, S. R. *Biopolymers (Pept. Sci.)* **2006**, *84*, 48−73.
(16) (a) Breuil, P.-A. R.; Patureau, F. W.; Reek, J. N. H. *Angew. Chem., Int. Ed.* **2009**, *48*, 2162−2165. (b) Breuil, P.-A. R.; Reek, J. N. H. *Eur. J. Org. Chem.* **2009**, 6225−6230.
(17) Dydio, P.; Rubay, C.; Gadzikwa, T.; Lutz, M.; Reek, J. N. H. *J. Am. Chem. Soc.* **2011**, *133*, 17176−17179.
(18) Review: Breitenlechner, S.; Selig, R.; Bach, T. In *Organocatalysis: Ernst Schering Foundation Symposium Proceedings*; Reetz, M. T., List, B., Jaroch, S., Weinmann, H., Eds.; Springer: Heidelberg, 2008; pp 255−279.
(19) Bauer, A.; Westkämper, F.; Grimme, S.; Bach, T. *Nature* **2005**, *436*, 1139−1140.
(20) (a) Müller, C.; Bauer, A.; Bach, T. *Angew. Chem., Int. Ed.* **2009**, *48*, 6640−6642. (b) Müller, C.; Maturi, M. M.; Bauer, A.; Cuquerella, M. C.; Miranda, M. A.; Bach, T. *J. Am. Chem. Soc.* **2011**, *133*, 16689−16697.
(21) (a) Albrecht, D.; Vogt, F.; Bach, T. *Chem.—Eur. J.* **2010**, *16*, 4284−4296. (b) Bakowski, A.; Dressel, M.; Bauer, A.; Bach, T. *Org. Biomol. Chem.* **2011**, *9*, 3516−3529. (c) Austin, K. A. B.; Herdtweck, E.; Bach, T. *Angew. Chem., Int. Ed.* **2011**, *50*, 8416−8419.
(22) Reviews: (a) Sonogashira, K. J. *Organomet. Chem.* **2002**, *653*, 46−49. (b) Negishi, E.; Anastasia, L. *Chem. Rev.* **2003**, *103*, 1979−2017. (c) Chinchilla, R.; Nájera, C. *Chem. Rev.* **2007**, *107*, 874−922. (d) Chinchilla, R.; Nájera, C. *Chem. Soc. Rev.* **2011**, *40*, 5084−5121.
(23) Reviews: (a) Moses, J. E.; Moorhouse, A. D. *Chem. Soc. Rev.* **2007**, *36*, 1249−1262. (b) Meldal, M.; Tornøe, C. W. *Chem. Rev.* **2008**, *108*, 2952−3015.
(24) (a) Voss, F.; Bach, T. *Synlett* **2010**, 1493−1496. (b) Voss, F.; Herdtweck, E.; Bach, T. *Chem. Commun.* **2011**, *47*, 2137−2139. (c) Voss, F.; Vogt, F.; Herdtweck, E.; Bach, T. *Synthesis* **2011**, 961−971.
(25) For the use of this skeleton in molecular recognition studies, see: (a) Rebek, J., Jr.; Askew, B.; Ballester, P.; Buhr, C.; Costero, S.; Jones, S.; Nemeth, D.; Williams, D. *J. Am. Chem. Soc.* **1987**, *109*, 6866−6867. (b) Jeong, K.-S.; Parris, K.; Ballester, P.; Rebek, J., Jr. *Angew. Chem., Int. Ed.* **1990**, *29*, 555−556. (c) Jeong, K. S.; Tjivikua, T.; Muehldorf, A.; Deslongchamps, G.; Famulok, M.; Rebek, J., Jr. *J. Am. Chem. Soc.* **1990**, *113*, 201−209.
(26) Fackler, P.; Berthold, C.; Voss, F.; Bach, T. *J. Am. Chem. Soc.* **2010**, *132*, 15911−15913.
(27) For the use of this skeleton in molecular recognition studies, see: (a) Lonergan, G. D.; Riego, J.; Deslongchamps, G. *Tetrahedron Lett.* **1996**, *37*, 6109−6112. (b) Lonergan, D. G.; Halse, J.; Deslongchamps, G. *Tetrahedron Lett.* **1998**, *39*, 6865−6868. (c) Lonergan, D. G.; Deslongchamps, G. *Tetrahedron* **1998**, *54*, 14041−14052.
(28) Kemp, D. S.; Petrakis, K. S. *J. Org. Chem.* **1981**, *46*, 5140−5143.
(29) Corwin, L. R.; McDaniel, D. M.; Bushby, R. J.; Berson, J. A. J. *Am. Chem. Soc.* **1980**, *102*, 276−287.
(30) Sonogashira, K.; Tohda, Y.; Hagihara, N. *Tetrahedron Lett.* **1975**, *16*, 4467−4470.
(31) Review on ruthenium porphyrin complexes: Simmoneaux, G.; Le Maux, P. *Coord. Chem. Rev.* **2002**, *228*, 43−60.
(32) For the functionalization of porphyrins, see: (a) Senge, M. O.; Shaker, Y. M.; Pintea, M.; Ryppa, C.; Hatscher, S. S.; Ryan, A.; Sergeeva, Y. *Eur. J. Org. Chem.* **2010**, 237−258. (b) Senge, M. O. *Chem. Commun.* **2011**, *47*, 1943−1960.
(33) Liddell, P. A.; Gervaldo, M.; Bridgewater, J. W.; Keirstead, A. E.; Lin, S.; Moore, T. A.; Moore, A. L.; Gust, D. *Chem. Mater.* **2008**, *20*, 135−142.
(34) For pioneering contributions to the enantioselective, transition metal catalyzed epoxidation of olefins, see: (a) Katsuki, T.; Sharpless, K. B. J. *Am. Chem. Soc.* **1980**, *102*, 5974−5976. (b) Groves, J. T.; Myers, R. S. J. *Am. Chem. Soc.* **1983**, *105*, 5791−5796. (c) Hanson, R. M.; Sharpless, K. B. J. *Org. Chem.* **1986**, *51*, 1922−1925. (d) Zhang, W.; Loebach, J. L.; Wilson, S. R.; Jacobsen, E. N. J. *Am. Chem. Soc.* **1990**, *112*, 2801−2803. (e) Irie, R.; Noda, K.; Ito, Y.; Matsumoto, N.; Katsuki, T. *Tetrahedron Lett.* **1990**, *31*, 7345−7348.

(35) Shanmugan, P.; Palaniappan, R. *Z. Naturforsch.* **1973**, *28*, 196−199.
(36) (a) Wittig, G.; Schöllkopf, U. *Chem. Ber.* **1954**, *87*, 1318−1330. (b) Hollywood, F.; Suschitzky, H. *Synthesis* **1982**, 662−665.
(37) El-Sayed, O. A.; Aboul-Enein, H. Y. *Arch. Pharm. Pharm. Med. Chem.* **2001**, *334*, 117−120.
(38) Tsoungas, P. G.; Searcey, M. *Tetrahedron Lett.* **2001**, *42*, 6589−6592.
(39) (a) Higuchi, T.; Ohtake, H.; Hirobe, M. *Tetrahedron Lett.* **1989**, *30*, 6545−6548. (b) Ohtake, H.; Higuchi, T.; Hirobe, M. *Heterocycles* **1995**, *40*, 867−903.
(40) For the epoxidation of 3-styrylquinolones, which was catalyzed by a chiral Ru-pybox complex and which proceeded with low enantioselectivity, see ref 24c.
(41) (a) Schwab, P.; Grubbs, R. H.; Ziller, J. W. *J. Am. Chem. Soc.* **1996**, *118*, 100−110. (b) Trnka, T. M.; Grubbs, R. H. *Acc. Chem. Res.* **2001**, *34*, 18−29. (c) Arrayas, R. G.; Alcudia, A.; Liebeskind, L. S. *Org. Lett.* **2001**, *3*, 3381−3384.
(42) (a) Groves, J. T.; Quinn, R. J. *Am. Chem. Soc.* **1985**, *107*, 5790−5792. (b) Groves, J. T.; Quinn, R. J. *Inorg. Chem.* **1984**, *23*, 3844−3846.
(43) (a) Gross, Z.; Ini, S.; Kapon, M.; Cohen, S. *Tetrahedron Lett.* **1996**, *37*, 7325−7328. (b) Gross, Z.; Ini, S. *J. Org. Chem.* **1997**, *62*, 5514−5521. (c) Frauenkron, M.; Berkessel, A. *J. Chem. Soc., Perkin Trans. 1* **1997**, 2265−2266. (d) Lai, T.-S.; Zhang, R.; Cheung, K.-K.; Kwong, H.-L.; Che, C.-M. *Chem. Commun.* **1998**, 1583−1584. (e) Lai, T.-S.; Kwong, H.-L.; Zhang, R.; Che, C.-M. *J. Chem. Soc., Dalton Trans.* **1998**, 3559−3564. (f) Ini, S.; Gross, Z. *Org. Lett.* **1999**, *1*, 2077−2080. (g) Zhang, R.; Yu, W.-Y.; Lai, T.-S.; Che, C.-M. *Chem. Commun.* **1999**, 409−410. (h) Zhang, R.; Yu, W.-Y.; Wong, K.-Y.; Che, C.-M. *J. Org. Chem.* **2001**, *71*, 8145−8153. (i) Zhang, J.-L.; Liu, Y.-L.; Che, C.-M. *Chem. Commun.* **2002**, 2906−2907. (j) Le Maux, P.; Lukas, M.; Simonneaux, G. *J. Mol. Catal. A: Chem.* **2003**, *206*, 95−103. (k) Berkessel, A.; Kaiser, P.; Lex, J. *Chem.—Eur. J.* **2003**, *9*, 4746−4756.
(44) Reviews: (a) Meunier, B. *Chem. Rev.* **1992**, *92*, 1411−1456. (b) Rose, E.; Andrioletti, B.; Zrig, S.; Quelquejeu-Ethève, M. *Chem. Soc. Rev.* **2005**, *34*, 573−583. (c) Che, C.-M.; Huang, J.-S. *Chem. Commun.* **2009**, 3996−4015.
(45) Zhao, Y.; Truhlar, D. G. *J. Chem. Phys.* **2006**, *125*, 194101−1−194101−18.
(46) Dolg, M.; Wedig, U.; Stoll, H.; Preuss, H. *J. Chem. Phys.* **1987**, *86*, 866−872.
(47) Hehre, W. J.; Radom, L.; Schleyer, P. v. R.; Pople, J. A. *Ab Initio Molecular Orbital Theory*; Wiley: New York, 1986.
(48) Frisch, M. J.; Trucks, G. W.; Schlegel, H. B.; Scuseria, G. E.; Robb, M. A.; Cheeseman, J. R.; Scalmani, G.; Barone, V.; Mennucci, B.; Petersson, G. A.; Nakatsuji, H.; Caricato, M.; Li, X.; Hratchian, H. P.; Izmaylov, A. F.; Bloino, J.; Zheng, G.; Sonnenberg, J. L.; Hada, M.; Ehara, M.; Toyota, K.; Fukuda, R.; Hasegawa, J.; Ishida, M.; Nakajima, T.; Honda, Y.; Kitao, O.; Nakai, H.; Vreven, T.; Montgomery, J. A., Jr.; Peralta, J. E.; Ogliaro, F.; Bearpark, M.; Heyd, J. J.; Brothers, E.; Kudin, K. N.; Staroverov, V. N.; Kobayashi, R.; Normand, J.; Raghavachari, K.; Rendell, A.; Burant, J. C.; Iyengar, S. S.; Tomasi, J.; Cossi, M.; Rega, N.; Millam, N. J.; Klene, M.; Knox, J. E.; Cross, J. B.; Bakken, V.; Adamo, C.; Jaramillo, J.; Gomperts, R.; Stratmann, R. E.; Yazyev, O.; Austin, A. J.; Cammi, R.; Pomelli, C.; Ochterski, J. W.; Martin, R. L.; Morokuma, K.; Zakrzewski, V. G.; Voth, G. A.; Salvador, P.; Dannenberg, J. J.; Dapprich, S.; Daniels, A. D.; Farkas, Ö.; Foresman, J. B.; Ortiz, J. V.; Cioslowski, J.; Fox, D. J. *Gaussian 09*, revision B.01; Gaussian, Inc.: Wallingford, CT, 2009.
(49) For the activation strain model of chemical reactivity, see: (a) Bickelhaupt, F. M. *J. Comput. Chem.* **1999**, *20*, 114−128. (b) van Zeist, W.-J.; Bickelhaupt, F. M. *Org. Biomol. Chem.* **2010**, *8*, 3118−3127.
(50) Sing, B. K.; Cavalluzzo, C.; Van Der Eycken, E.; Parmar, V. S.; De Maeyer, M.; Debyser, Z. *Eur. J. Org. Chem.* **2009**, *27*, 4589−4592.
(51) The compound was prepared by Suzuki cross-coupling from the respective bromide: Novartis A. G. WO2008/58967 A1, 2008 (see Supporting Information).
(52) The compound was prepared by Suzuki cross-coupling from the respective bromide: Wishka, D. G.; Walker, D. P.; Yates, K. M.; Reitz, S. C.; Jia, S.; Myers, J. K.; Olson, K. L.; Jacobsen, E. J.; Wolfe, M. L.; Groppi, V. E.; Hanchar, A. J.; Thornburgh, B. A.; Cortes-Burgos, L. A.; Wong, E. H. F.; Staton, B. A.; Raub, T. J.; Higdon, N. R.; Wall, T. M.; Hurst, R. S.; Walters, R. R.; Hoffmann, W. E.; Hajos, M.; Franklin, S.; Carey, G.; Gold, L. H.; Cook, K. K.; Sands, S. B.; Zhao, S. X.; Soglia, J. R.; Kalgutkar, A. S.; Arneric, S. P.; Rogers, B. N. *J. Med. Chem.* **2006**, *49*, 4425−4426 (see Supporting Information)..
(53) Node, M.; Nishide, K.; Shigeta, Y.; Obata, K.; Shiraki, H.; Kunishige, H. *Tetrahedron* **1997**, *53*, 12883−12984.
(54) Takami, K.; Yorimitsu, H.; Oshima, K. *Org. Lett.* **2004**, *6*, 4555−4558.
(55) Stoermer, R.; Stockmann, R. *Chem. Ber.* **1914**, *47*, 1786−1793.
(56) The compound was prepared from the respective allylalcohol: Pavlakos, E.; Georgiou, T.; Tofi, M.; Montagnon, T.; Vassilikogiannakis, G. *Org. Lett.* **2009**, *11*, 4556−4559 (see Supporting Information).

■ NOTE ADDED AFTER ASAP PUBLICATION

The toc/abstract graphic was incorrect in the version published ASAP July 23, 2012. The correct version reposted August 1, 2012.